

Article

# Partial Discharge of Needle-Plane Defect in Oil-Paper Insulation under AC and DC Combined Voltages: Developing Processes and Characteristics

Jiantao Sun <sup>1</sup>, Xining Li <sup>2</sup>, Lingyu Zhu <sup>2,\*</sup> , Shengchang Ji <sup>2</sup> and Yanjie Cui <sup>2</sup>

<sup>1</sup> China Electric Power Research Institute, Beijing 100192, China; sunjt@epri.sgcc.com.cn

<sup>2</sup> State Key Laboratory of Electrical Insulation and Power Equipment, Xi'an Jiaotong University, Xi'an 710049, China; dalianlxn@stu.xjtu.edu.cn (X.L.); jsc@xjtu.edu.cn (S.J.); xjtucyj@126.com (Y.C.)

\* Correspondence: zhuly102@gmail.com; Tel.: +86-186-2952-9085

Received: 28 September 2017; Accepted: 27 October 2017; Published: 1 November 2017

**Abstract:** Partial discharge (PD) behaviors of oil-paper insulation is distinctive in AC and DC combined electric fields in converter transformers from PD behaviors in pure AC or DC electric fields. The present study focuses on the PD developing processes and characteristics of oil-paper insulation systems with needle-plane defects under different AC/DC proportions. The degradation of oil-paper insulation can be accelerated by PD pulses incurred by needle-plane defects. AC-DC combined voltages are applied to the needle-plane defect model simultaneously in the established experimental platform, and the proportions of AC/DC voltages are decided according to the cases in actual converter transformers. The developing processes from the initiation of partial discharge until final breakdown were observed for each AC/DC proportion. PD parameters and patterns were acquired by a detector using the pulse current method. The test results indicate that the inception and breakdown voltages increase with the increase of the DC component in AC-DC combined voltages. However, pulse repetition rate and amplitude of PD shows a descending trend when AC/DC proportion decreases. Meanwhile, the PD recurrence rate in the phase between 180° and 360° becomes higher than that in the phase between 0° and 180° at the initial stage as the DC proportion increases; high-amplitude discharges mainly occur in the phase range between 180° and 360° when the pressboard is close to breakdown. The current study is useful in further research on fault diagnosis in converter transformers.

**Keywords:** oil-paper insulation; converter transformer; partial discharge (PD); needle-plane defect; AC/DC proportion

## 1. Introduction

For the converter transformers used in HVDC (High Voltage Direct Current) transmission systems, the valve-side windings withstand complicated voltage stresses, which consist of AC, DC and harmonic waveforms [1,2]. Partial discharge (PD) activities under the AC-DC combined voltages are different from PDs in transformers of AC grids [3–9]. Furthermore, the proportion of AC and DC voltages are different at different positions of the winding. Different AC/DC proportions influence electrical properties of insulating oils and insulation paper, which may lead to different PD behaviors in oil-paper insulation system. Therefore, it is significant to interpret PD characteristics under AC-DC combined voltage with different proportions and provide the diagnosis basis distinguished with the insulation problem at different locations of converter transformers.

Much research has been concentrated on partial discharge characteristics of oil-paper insulation under AC-DC combined voltages [6–15]. The PD characteristics of different insulation conditions of pressboard under DC and AC-DC combined voltage are investigated in [10]. In [11], the effect of

space charge on the reliability of oil-paper insulation under HVDC stress is studied by using the PEA method. Typical phase-resolved PD distribution (PRPD) patterns, which can be used in fault mode recognition for converter transformers, are presented in [12]. The inception voltage under different ratios of AC-DC combined voltages were measured in [13]. The electric field distribution of oil-paper insulation systems was measured by the Kerr electro-optic effect under AC-DC combined voltage in [14]. In addition, in [15], the influences of AC/DC proportions on internal gas cavity discharge in oil-pressboard insulation are studied.

From the above literature review, little research concerns the effects of AC and DC voltage proportions on the partial discharge characteristic behavior of needle-plane defects in oil-pressboard insulations. Furthermore, the developing processes have not been described in previous studies. The considerable knowledge gap motivated us to conduct research on the PD developing process and characteristics of needle-plane defects in oil-paper insulation under AC-DC combined voltages. The paper is organized as follows. In Section 2, the needle-plane defect model was designed to simulate metallic protrusion insulation defects, which can generate PDs under AC-DC combined voltages with different proportion. The inception and breakdown voltages, statistical distributions and typical parameters of PDs were analyzed in Sections 3 and 4. Section 5 explains the experimental results from the theoretical point of view. The present study can provide a basis for the realization of fault diagnosis and condition monitoring of HVDC converter transformers.

## 2. Experimental Setup of the PD Test under AC-DC Combined Voltage

### 2.1. Test Model

The needle-plane defect model for tests is shown in Figure 1a, which can simulate the existence of inhomogeneous electric fields in converter transformers. The needle electrode is a stainless steel needle with a curvature radius approximate to 70  $\mu\text{m}$ . Plane electrode is made of brass with all edges well-polished in order to avoid unexpected discharges. The whole defect model is placed in a synthetic glass box filled with transformer oil to simulate metallic protrusion insulation defect. Make sure that the whole defect model is entirely immersed in the oil in order to prevent interferential discharges.

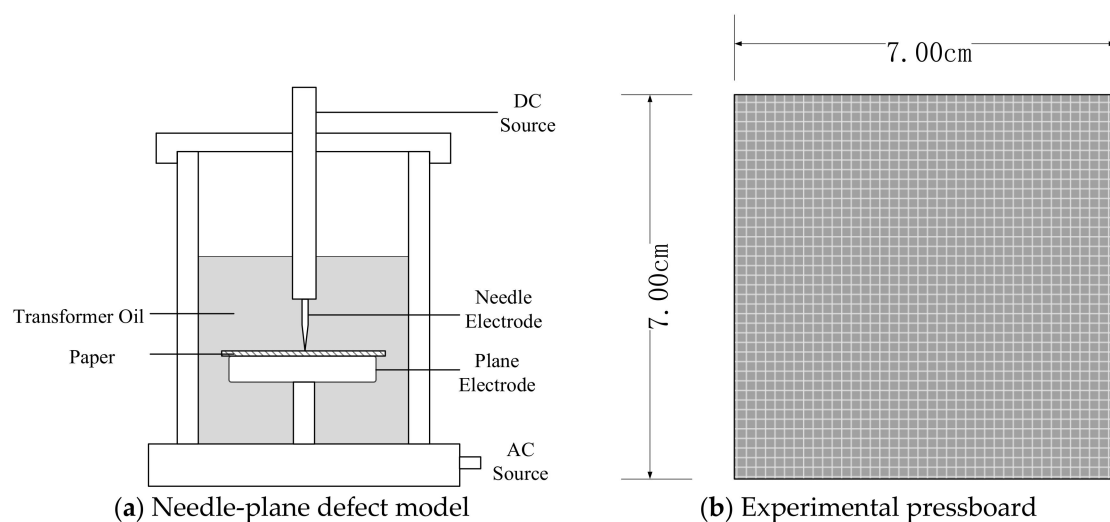


Figure 1. Experimental specimen.

As shown in Figure 1b, pressboards with a thickness of 1 mm and a size of 7 cm  $\times$  7 cm need to be put into a vacuum drying chamber, constantly dried for 48 h at 110  $^{\circ}\text{C}$  in an argon environment in order to remove moisture inside pressboards. The pressboards are immersed in transformer oil and

dried for 24 h at 60 °C in order to remove both moisture and air before being placed between two metal electrodes [16].

## 2.2. Test Circuit

The PD experiment circuit in the laboratory was founded and calibrated by the method suggested in [3,17,18]. As presented in Figure 2, the voltage sources include a DC voltage source and an AC voltage source. In Figure 2,  $R_{ac}$  and  $R_{dc}$  are current-limiting resistances of AC and DC circuits, with the same resistance value of 30 k $\Omega$ .  $C_f$  is a 10 nF DC filter capacitor, which guarantees the ripple factor of DC source smaller than 0.5%.  $C_0$  is the coupling capacitor, with a capacitance of 800 pF. PD signal is acquired by PD detector through the detection impedance  $Z_m$ . The voltage applied on the defect model was detected by an HV probe, therefore its waveform can be collected by a digital oscilloscope. For all experiments, the voltage was raised in steps of about 50 V/s. Discharge pulse signals were acquired every 5 min during experiments, especially when the parameters of PDs changed dramatically. Due to the detection frequency bandwidth of the PD detector is 1 MHz, which is higher than the frequency of noise signal generated by enormous switching in HVDC equipment. Thus, the influence of the high noise level in HVDC system can be neglected in the current study. The tests were performed in an electromagnetic-shielded laboratory environment. The background noise of environment was about 10 pC.

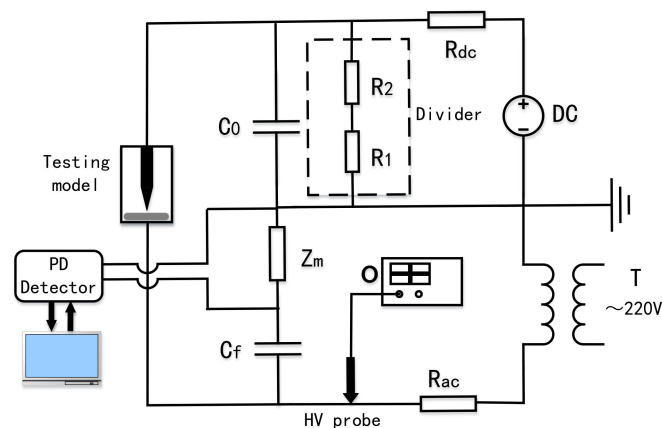


**Figure 2.** Partial discharge measurement system.

## 2.3. Voltage Application Method

According to paper [15], four different proportions between the effective value of AC voltage and the mean value of DC voltage at the valve side windings of converter transformers are obtained, which are 1:1, 1:3, 1:5, and 1:7 respectively. The step-up voltage application method is used to acquire sufficient measurement data efficiently. This method is capable of damaging the oil-paper insulation in the same extent compared with the constant voltage application method [19–21].

The proportion between the AC voltage and DC mean voltages were maintained during tests. AC and DC voltages were increased by one step every 5 min until specimen breakdown, and each step is 4–8 kV. PD parameters are recorded to study the influence of different proportion of AC and DC combined voltages in terms of both partial discharge phenomena and statistical characteristics. The waveform of applied voltage and voltage step-up method are shown in Figures 3 and 4.

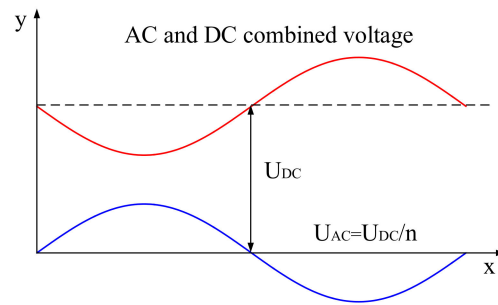


Figure 3. Applied voltage waveform.

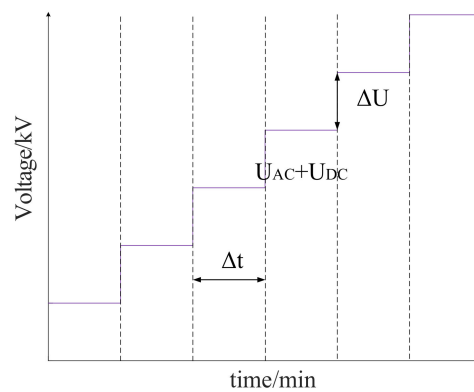


Figure 4. Voltage step-up method.

### 3. PD Developing Processes for Different AC/DC Proportions

The PD developing processes from the initial stage to the breakdown of the pressboard under different AC/DC proportions are investigated in this section. The applied voltage is increased step by step, and PD parameters and patterns are analyzed for each stage of the PD development. It should be mentioned that in the case of AC-DC combined voltage, partial discharge inception voltages (PDIV) are defined as the mean value of three measurement results of the sum of AC effective voltage and DC voltage when repetitive PD pulses are firstly detected during the voltage boosting. All the tests were repeated three times in the investigation to obtain reliable test results.

#### 3.1. AC/DC Proportion of 1:1

PDIV under AC/DC proportion of 1:1 is about 14 kV, when AC effective value and DC mean value equal to 7 kV. Both pulse repetition rate (the mean value of PD pulses per second [3]) and mean PD amplitude increase with the increase of applied voltage, as shown in Figure 5. In the partial discharge initial stage, the magnitudes and frequencies of PDs are small. Then the growth rate of PD pulse number becomes higher with the applied voltage, especially since the AC and DC voltage increase to 15 kV. The repetition rate stops increasing and stays at around 270 times per second a short period before breakdown, which is pre-breakdown stage. During the whole process, mean PD amplitude increases steadily in a constant augment rate. The breakdown voltage of the pressboard is 42 kV.

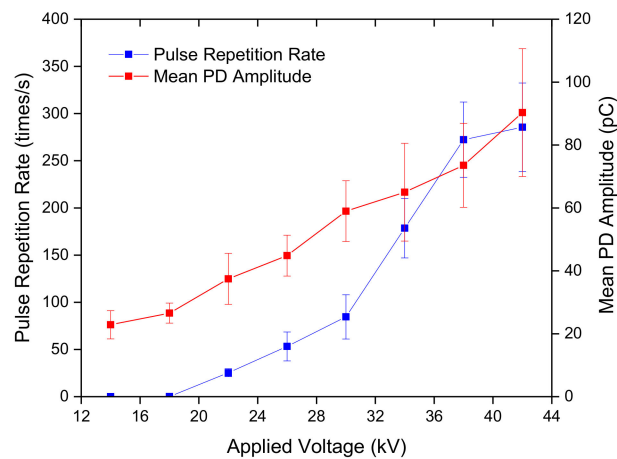


Figure 5. PD parameters under AC/DC proportion of 1:1.

Figure 6 shows PD phase-resolved distributions of the needle-plane defect in oil-paper insulation under 1:1 AC-DC combined voltages. At the AC/DC proportion of 1:1, partial discharges at the initial stage mainly occur between  $0^\circ$  and  $90^\circ$  and  $180^\circ$  and  $270^\circ$ , and pulse repetition rates in positive and negative half cycle are nearly the same. Figure 6b shows that the partial discharges of pre-breakdown stage distribute all over the phase intervals, and lots of high amplitude PDs appear in the phase between  $180^\circ$  and  $360^\circ$ .

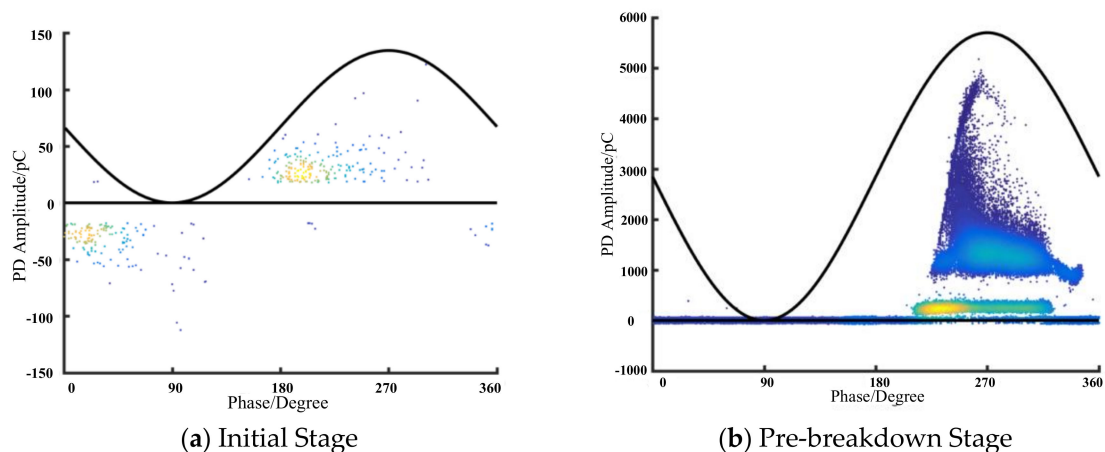
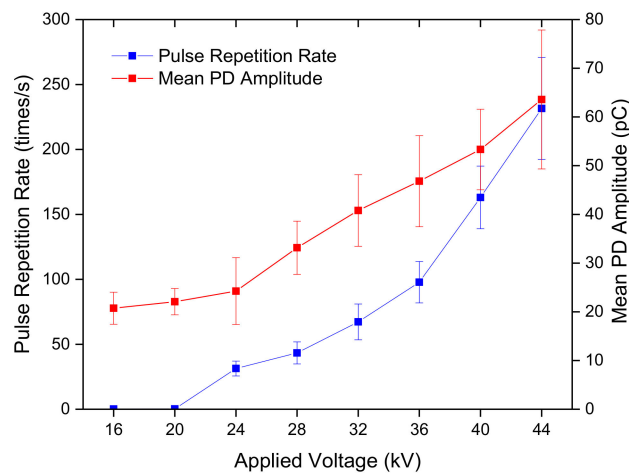


Figure 6. PRPD patterns under AC/DC proportion of 1:1.

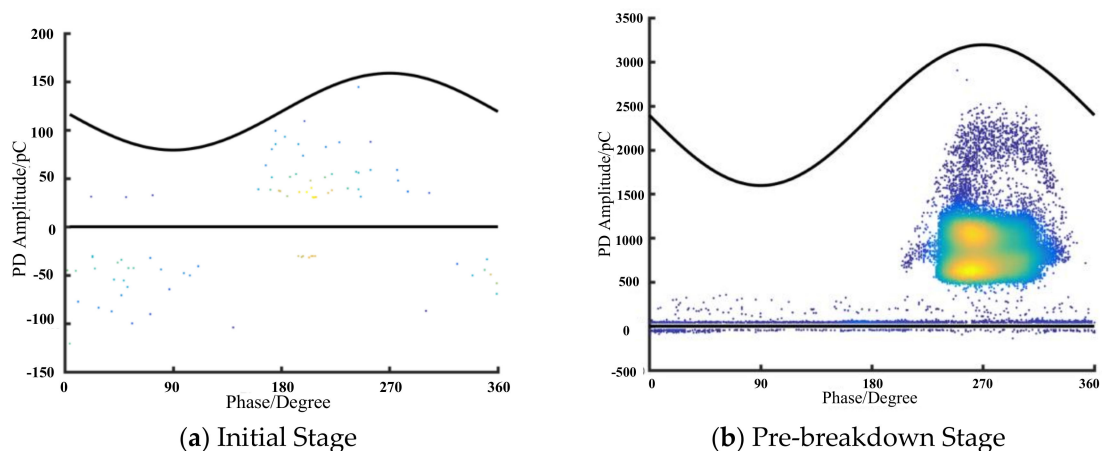
### 3.2. AC/DC Proportion of 1:3

Figure 7 shows the relationships between the applied voltage and pulse repetition rate, as well as mean PD amplitude, under AC/DC proportion of 1:3. Partial discharges occur when applied DC voltage increases to 12 kV and AC voltage to 4 kV. Pulse repetition rate and mean PD amplitude are very small at the initial stage, which are less than 1 time per second and 20 pC, respectively. Then, since voltage is increased to about 24 kV, these two parameters show an obvious growing trend with the increase of applied voltage until the breakdown of the specimen, at the voltage of 44 kV. In the pre-breakdown stage, pulse repetition rate is around 230 times per second, while mean PD amplitude is about 65 pC.



**Figure 7.** PD parameters under AC/DC proportion of 1:3.

When AC/DC proportion equals to 1:3, PD pulses under PDIV mainly happens in the phase intervals between  $10^\circ$  and  $90^\circ$  and between  $180^\circ$  and  $260^\circ$ , as shown in Figure 8a. The phase distribution is similar to that of 1:1. The pulse repetition rates in the phase between  $180^\circ$  and  $360^\circ$  are higher compared with those in the phase between  $0^\circ$  and  $180^\circ$ . The PRPD pattern in the pre-breakdown stage shown in Figure 8b indicates that high-magnitude PD pulses still mainly occur from  $180^\circ$  to  $360^\circ$ , and PD pulses distribute on all phases interval.



**Figure 8.** PRPD patterns under AC/DC proportion of 1:3.

### 3.3. AC/DC Proportion of 1:5

PD initial stage under 1:5 AC/DC proportion starts when AC-DC combined voltage is 18 kV. In Figure 9, both pulse repetition rate and mean PD amplitude increase in a constant rate as applied voltage rises when the applied voltage is lower than 42 kV. However, pulse repetition rate increases sharply since applied voltage is higher than 42 kV, while PD magnitude keeps the former growing rate. As pressboard continues to degrade, mean PD amplitude finally rises to 50 pC in the pre-breakdown stage. In this stage, pulse repetition rate is about 180 times per second. Pressboards breakdown when AC voltage at 8 kV and DC voltage at 40 kV.

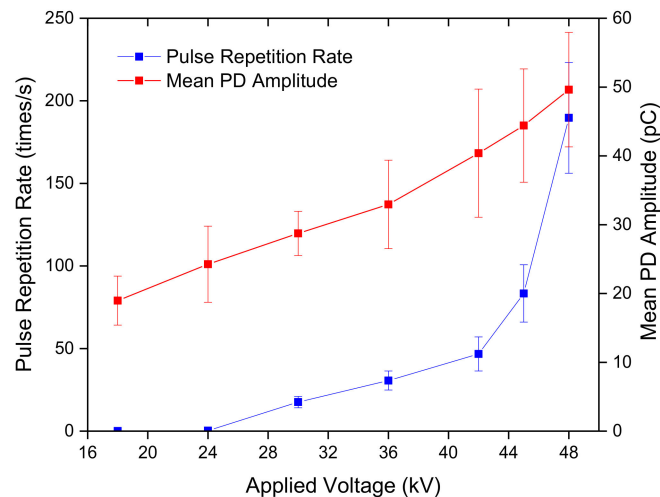


Figure 9. PD parameters under AC/DC proportion of 1:5.

PD phase distributions at the initial stage under 1:5 AC/DC proportion are much different change from the previous two proportions as shown in Figure 10a: only a few PDs occur in the phase between  $0^\circ$  and  $180^\circ$ , and PDs mainly concentrate between  $200^\circ$  and  $320^\circ$ . During pre-breakdown stage, high-amplitude PDs still only take place in the phase between  $180^\circ$  and  $360^\circ$ , as shown in Figure 10b. However, low-amplitude PD pulses occur on all phase interval from  $0^\circ$  to  $360^\circ$ , which is different from PD phenomena in initial stage.

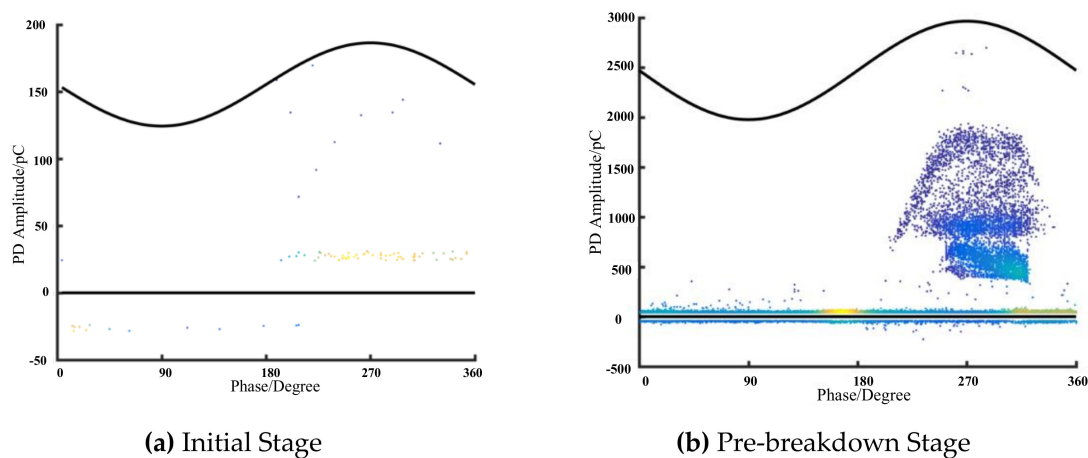


Figure 10. PRPD patterns under AC/DC proportion of 1:5.

#### 3.4. AC/DC Proportion of 1:7

The PDIV under the AC/DC proportion of 1:7 has an effective AC voltage of 2.5 kV and average DC voltage of 17.5 kV. Both pulse repetition rate and mean PD amplitude increase slowly at the PD initial stage, as presented in Figure 11. However, pulse repetition rate increases sharply once the applied voltage is over 44 kV. In the pre-breakdown stage of the specimen, mean PD amplitude is about 35 pC, while PD pulses frequency reaches 120 times per second. After the final pre-breakdown stage, the pressboard breaks down when the value of AC-DC combined voltage equals to 52 kV.

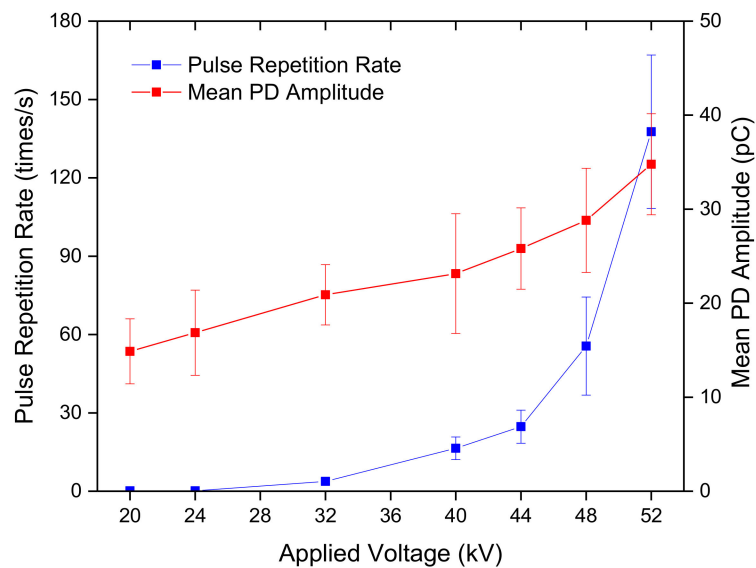


Figure 11. PD parameters under AC/DC proportion of 1:7.

As the AC/DC proportion decreases to the proportion of 1:7, the applied voltage is more like the DC voltage. PD pulses at the initial stage all happen in the phase between  $250^\circ$  and  $350^\circ$ , and there is no PDs occur in the phase between  $0^\circ$  and  $180^\circ$ , as shown in Figure 12a. When PD developing process comes to the pre-breakdown stage, PD pulses wrap all phase range between  $0^\circ$  and  $360^\circ$ . In this stage, high magnitude PDs happen from  $180^\circ$  to  $360^\circ$ .

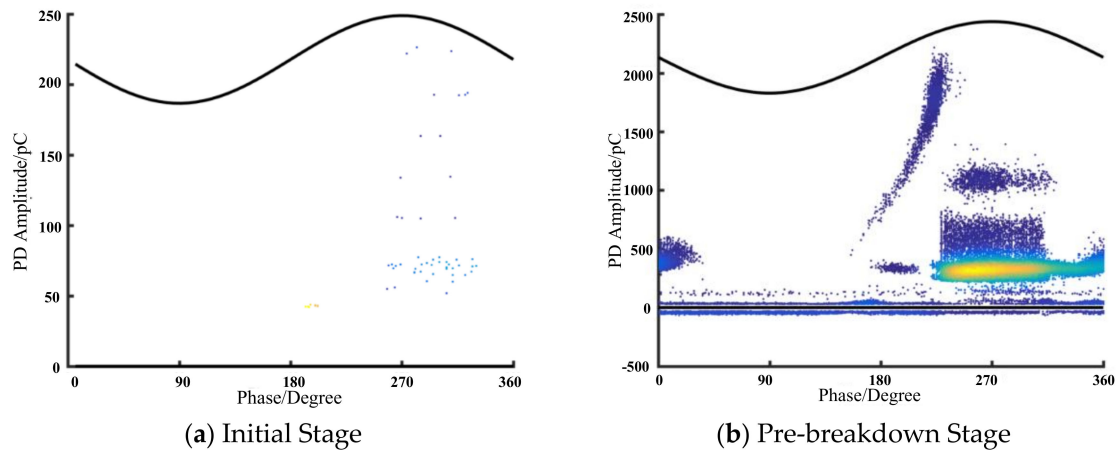


Figure 12. PRPD patterns under AC/DC proportion of 1:7.

During the initial stage, some bubble columns were formed near the tip of the needle by some small floating bubbles induced by partial discharge of charged impurities in the oil. PD energy will break the molecular bond of both oil and pressboard, vaporize oil and finally form bubbles. In the pre-breakdown stage, as the bubble columns formed from the plane electrode to the needle tip fractured by high-amplitude discharge pulses, discharging paths inside the pressboard appear and increase the current passing through the pressboard. This phenomenon has a harmful erosive effect to the pressboard, which results in the breakdown of the insulation system.

#### 4. PD Characteristics under Different AC/DC Proportions

##### 4.1. PDIVs and Breakdown Voltages under Different AC/DC Proportions

The influence of AC/DC proportions on PDIV and breakdown voltage induced by the needle-plane defect is summarized in Table 1.

**Table 1.** Relationship between PDIV and breakdown voltage and AC/DC proportions.

AC/DC Proportion	PDIV/kV			Breakdown Voltage/kV		
	AC	DC	Combined	AC	DC	Combined
1:1	8.5	8.5	17	21	21	42
1:3	4.5	13.5	18	11	33	44
1:5	3.2	16	19.2	8	40	48
1:7	2.5	17.5	20	6.5	45.5	52

Figure 13 shows PDIVs and breakdown voltages under different proportions of AC and DC combined voltage. The PDIV at the AC/DC proportion of 1:1 is the minimum. With the decrease of AC/DC proportions, which means DC component increases, PDIV of the needle-plane defect model increases. In this circumstance, AC component steadily decreases when DC component increases constantly. At the AC/DC proportion of 1:1, breakdown voltage of the pressboard is also the minimum. Breakdown voltage significantly increases when the AC/DC proportion decreases, especially for the AC/DC proportion of 1:7. It can be concluded that the breakdown voltage increases gradually when DC component dominates in AC-DC combined voltages.

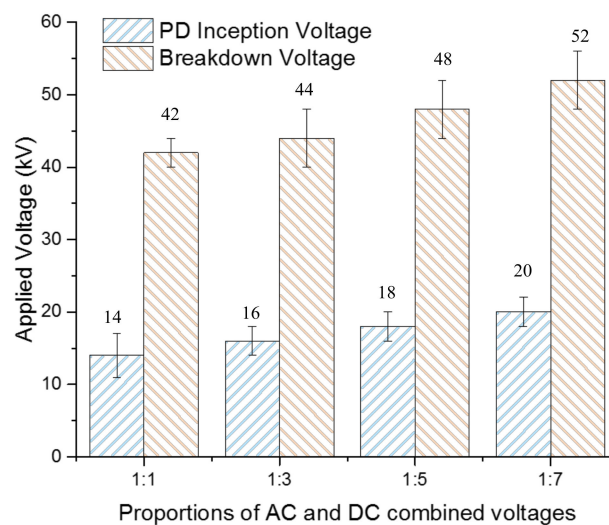


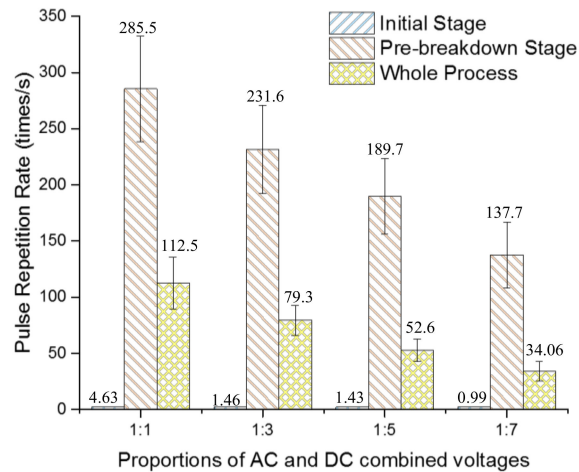
**Figure 13.** Relationship between PDIV and breakdown voltage and AC/DC proportions.

##### 4.2. Pulse Repetition Rate under Different AC/DC Proportions

Table 2 and Figure 14 reports the relationship between pulse repetition rate and proportions of AC and DC combined voltage at the initial stage, pre-breakdown stage, and whole PD developing process. The data was normalized for comparison convenience. At the PD initial stage, pulse repetition rates are low for all the AC/DC proportions, which are less than once per second. Pulse repetition rate becomes much higher during pre-breakdown stage. The value reaches over 280 under the 1:1 AC-DC combined voltage, and it decreases constantly with the decrease of the AC/DC proportion. As for the whole PD process, pulse repetition rate also decreases with AC/DC proportion, which is similar to the case at initial and pre-breakdown stages.

**Table 2.** Relationship between pulse repetition rate and AC/DC proportions.

AC/DC Proportion	Initial Stage	Pre-Breakdown Stage	Whole Process
1:1	4.63	285.50	112.45
1:3	1.46	231.57	79.34
1:5	1.43	189.68	52.61
1:7	0.99	137.66	34.06

**Figure 14.** Relationship between pulse repetition rate and AC/DC proportions.

### 4.3. PD Amplitude under Different AC/DC Proportions

#### 4.3.1. Trend of Max PD Amplitude

Table 3 and Figure 15 shows the changes in max PD amplitude at the initial stage and the pre-breakdown stage of the needle-plane defect in oil-paper insulation under different AC/DC proportions. Max PD amplitude at the initial stage increases a little as AC/DC proportion decreases, from about 170 pC to 250 pC. Max PD amplitude at the pre-breakdown also decreases with the decrease of the AC/DC proportion. However, the max PD amplitude shows more stochastic performance, and the variances of the experimental results are relatively high. Thus, max PD changes with the decrease of the AC/DC proportion in a general descend trend, but not very strictly, as shown in Figure 15.

**Table 3.** Relationship between Max PD amplitude AND AC/DC proportions.

AC/DC Proportion	Initial Stage/pC	Pre-Breakdown Stage/pC
1:1	173.4	5644.5
1:3	176.22	3303.3
1:5	251.94	2714.2
1:7	255.18	2466.4

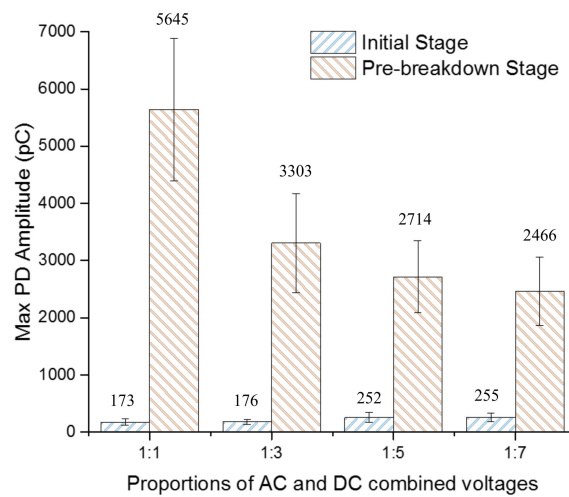


Figure 15. Relationship between max PD amplitude and AC/DC proportions.

### 4.3.2. Trend of Mean PD Amplitude

The changing trend of mean PD amplitude given different proportions of AC and DC combined voltages is displayed in Table 4 and Figure 16. Mean PD amplitude at the partial discharge initial stage decreases a little as the AC/DC proportion decreases. While the mean PD amplitude at the pre-breakdown stage decreases rapidly when the AC/DC proportion drops in the range of 1:1 to 1:7. The changing trends of the mean PD magnitudes with the AC/DC proportions are similar for the whole partial discharge process.

Table 4. Relationship between mean PD amplitude and AC/DC proportions.

AC/DC Proportion	Initial Stage/pC	Pre-Breakdown Stage/pC	Whole Process/pC
1:1	22.85	90.32	52.45
1:3	20.73	63.59	38.09
1:5	18.96	49.62	34.19
1:7	14.88	34.77	23.6

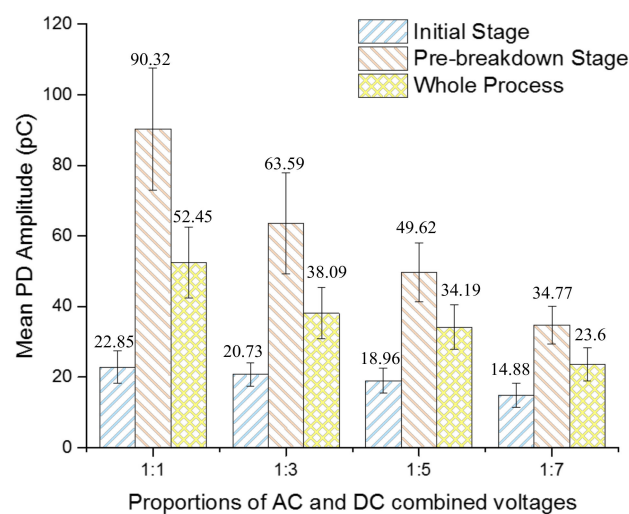


Figure 16. Relationship between mean PD amplitude and AC/DC proportions.

#### 4.3.3. Trend of Total Discharge Amplitude

Table 5 and Figure 17 present the influence of AC/DC proportion on the total discharge amplitudes. The total discharge amplitudes are normalized and calculated for 1 min. At the initial stage, the total discharge amplitude decreases with the AC/DC proportion. Total discharge amplitudes are less than 4 nC when the AC/DC proportion decreases below 1:3. On the other hand, the total discharge magnitudes at the pre-breakdown stage also decreases with the AC/DC proportion, and the decrease rate is higher compared with the initial stage.

**Table 5.** Relationship between total discharge amplitude and AC/DC proportions.

AC/DC Proportion	Initial Stage/nC	Pre-Breakdown Stage/nC
1:1	5.05	507.36
1:3	3.51	187.45
1:5	2.26	110.54
1:7	2.03	80.12

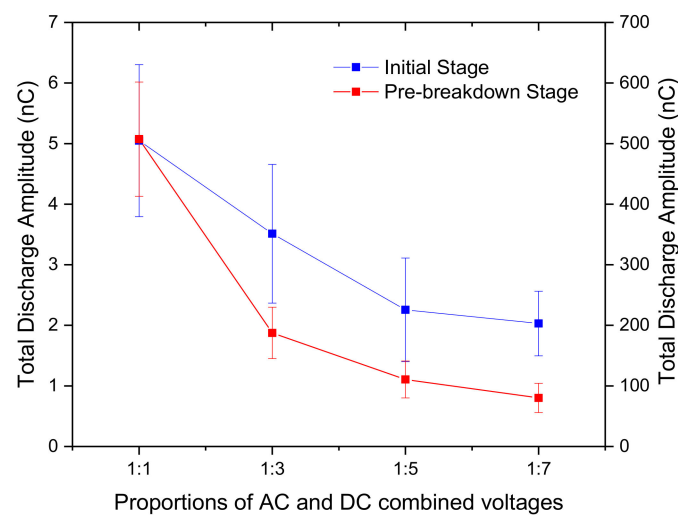


**Figure 17.** Relationship between total discharge amplitude and AC/DC proportions.

#### 4.4. PD Phase Distribution under Different AC/DC Proportions

Table 6 and Figure 18 compare the partial discharge phase-resolved distributions under different AC/DC proportions of the needle-plane defect. In the initial stage, the partial discharge pulses phase distributions gradually concentrate toward between the phase of  $180^\circ$  and  $360^\circ$  as the DC component in AC-DC combined voltage increases, and partial discharge pulses only occur in the phase between  $180^\circ$  and  $360^\circ$  when DC proportion is increased to 1:7. At the pre-breakdown stage, PRPD figures show that the distributions of the partial discharge pulses cover the whole phase intervals from  $0^\circ$  to  $360^\circ$ . However, high amplitude discharges only happen from  $200^\circ$  to  $310^\circ$ .

**Table 6.** Relationship between PD phase distribution AND AC/DC proportions ( $\phi/^\circ$ ).

AC/DC Proportion	Initial Stage		Pre-Breakdown Stage	
	Positive	Negative	Positive	Negative
1:1	0~80	160~250	-	210~320
1:3	10~60	160~250	-	230~310
1:5	10~30	200~340	150~180	250~310
1:7	-	260~320	-	220~360

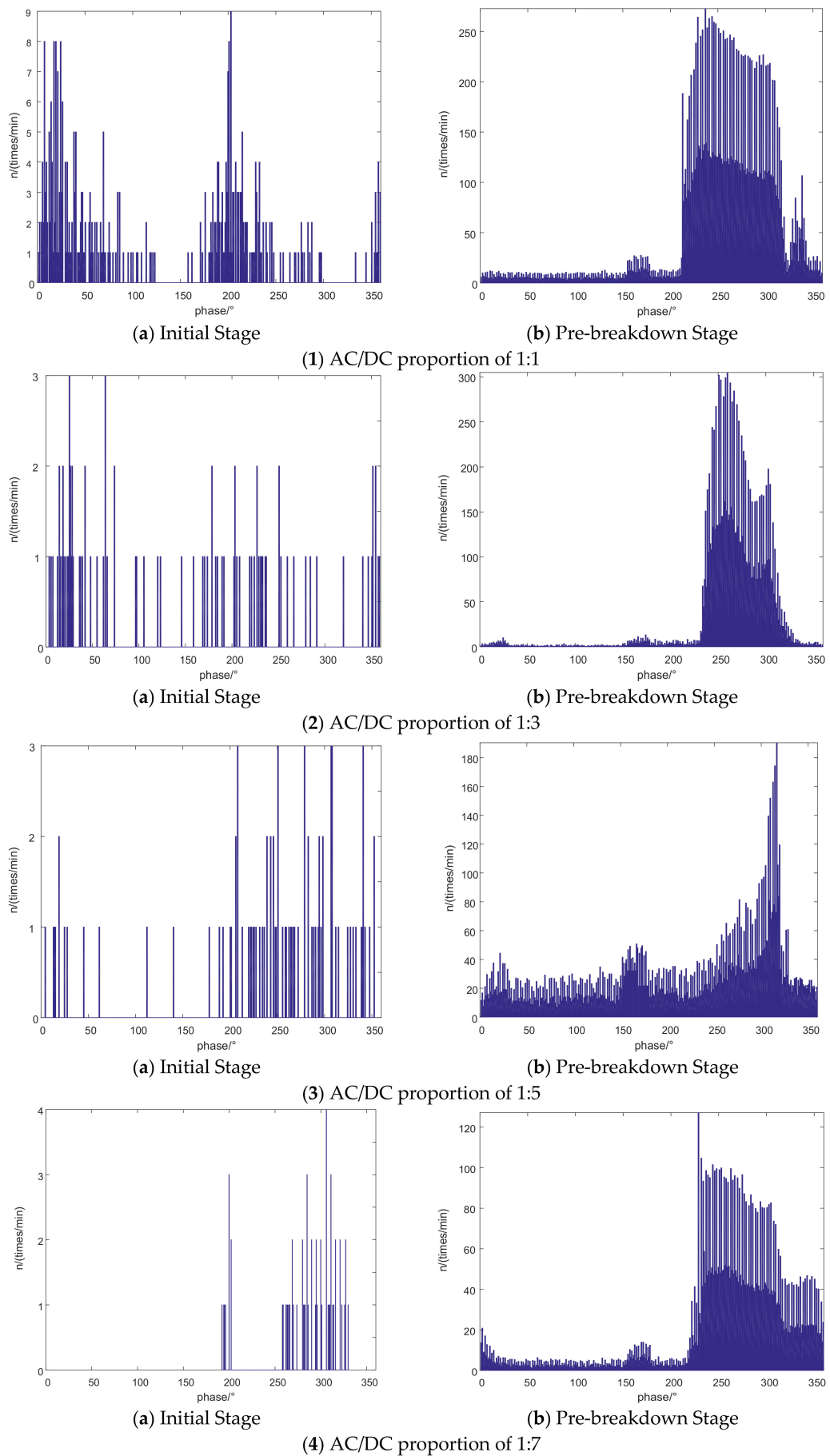


Figure 18. Phase distributions of PD pulses under different AC/DC proportions.

### 5. Discussions on the Influence of AC/DC Proportion

It was assumed that the partial discharges firstly occurred at the needle tip, which clings to microscopic holes among cellulose fibers on the surface of the pressboard. When applied voltage is low, only occasional discharges occur on the region where the needle touches pressboard. Space charges do not have an obvious effect on partial discharge.

#### 5.1. Analysis of Electric Filed Distribution

As these low-energy discharges cause the erosion of fibers on the tiny region under the needle on the surface of pressboard, the sunken region will be filled with transformer oil. Figure 19 presents the diagram of the needle-plane defect after a little damage on the surface of the pressboard. In Figure 19, 'a' represents the sunken region filled with oil, 'b' denotes the parallel remaining pressboard of 'a' after the damage and 'c' corresponds to the remaining pressboard.

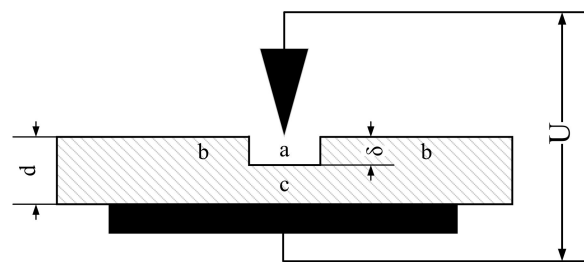


Figure 19. Diagram of the needle-plane defect in oil-paper insulation.

The equivalent circuit of the entire defect structure of oil-paper insulation under needle tip could be drawn as Figure 20. According to [22], the AC electric fields in the areas of 'a' and 'c' are decided by their dielectric coefficients, which is

$$\frac{E_{aac}}{E_{cac}} = \frac{U_{ab}/\delta}{U_c/(d - \delta)} = \frac{\epsilon_c}{\epsilon_a} \tag{1}$$

where  $\epsilon_c$  and  $\epsilon_a$  represent dielectric coefficients of the pressboard and the oil. As the dielectric coefficient of the pressboard is smaller than that of the oil ( $\epsilon_a \approx 2.2$  and  $\epsilon_c \approx 4.5$ ), the AC electric field intensity in oil  $E_a$  is higher than that of the pressboard  $E_c$ .

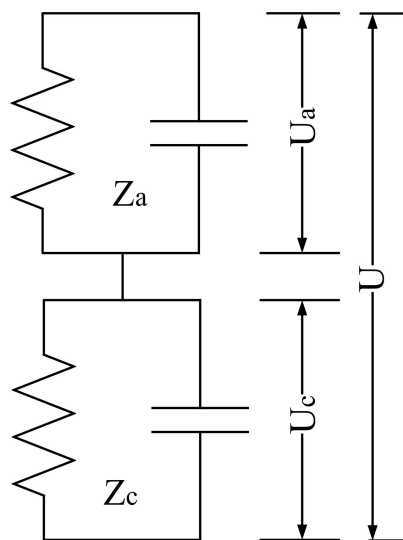


Figure 20. Diagram of equivalent circuit of the needle-plane defect.

For the DC electric field, the distribution of electric field intensity in the oil-paper insulation depends on their electric conductivities [23], which is

$$\frac{E_{\text{adc}}}{E_{\text{cdc}}} = \frac{\gamma_c}{\gamma_a} \quad (2)$$

where,  $\gamma_a \approx 10^{-13} \sim 10^{-15}$  is higher than  $\gamma_c \approx 10^{-16}$ . Equation (2) shows that the DC electric field withstand by the pressboard is higher than that in the oil.

### 5.2. The Influence of AC/DC Proportion on the PDIV and Breakdown Voltage

At the initial stage, repetitive PD pulses do not appear until AC-DC combined electric field intensity rises up to a certain extent. As shown in Table 1, AC electric field intensity decreases with the decrease of AC component in AC-DC combined voltage. Therefore, the intensity of the DC electric field needs to be increased to reach the condition of the initial discharge for the needle-plane defect, and DC component in combined voltages should be raised [24,25].

When it comes to the pre-breakdown stage, the accumulation of the space charges on the surface of the pressboard form an inverse electric field, which suppresses the principal electric field inside the pressboard. As a result, DC components need to increase to weaken the effect of the inverse electric field and make pressboard breakdown. Furthermore, the accumulation of space charges becomes stronger when the DC component of AC-DC combined voltage increases, which results in an increasing inverse electric field intensity. The DC component in AC-DC combined voltages should be increased to meet the breakdown condition of the pressboard [26].

Figure 21 suggests that the space charges motivated by PDs will form an electric field  $E_r$ , which is opposite to the direction of  $E_{\text{dc}}$ . This phenomenon not only reduces the pulse repetition rate, but also limits the discharge amplitudes during the whole process.

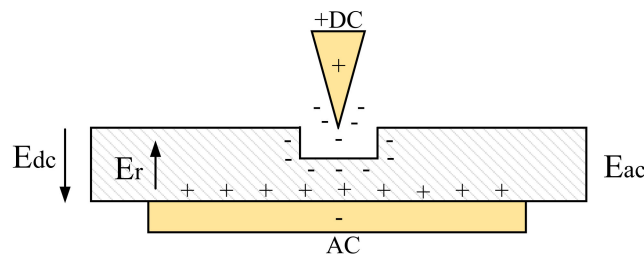


Figure 21. Diagram of the electric field of the needle-plane defect.

### 5.3. The Influence of AC/DC Proportion on the PRPD Patterns

At the initial stage, the amount of space charges generated by PD pulses is not much. When AC/DC proportion is 1:1 and 1:3, higher AC components in combined voltages will neutralize most of space charges inside the pressboards. Hence the effect of the inverse electric field  $E_r$  on the entire electric field is reduced, which results in PD pulses occurring in the phase from  $0^\circ$  to  $360^\circ$ , as shown in Figures 6 and 8. When AC/DC proportion decreases to 1:5 and 1:7, DC component takes a dominant role in the entire electric field. The entire electric field reaches its peak value when AC voltage is in the phase between  $180^\circ$  and  $360^\circ$ . Thus, partial discharges take place around  $270^\circ$  at first in Figures 10 and 12 [25,26].

When it comes to the pre-breakdown stage, as applied voltage is in a very high level, PDs happen in all phases from  $0^\circ$  to  $360^\circ$ . Furthermore, as the entire electric field in the phase between  $180^\circ$  and  $360^\circ$  almost reaches the specimen breakdown condition, high-amplitude discharges only occur in the phase ranging mainly from  $200^\circ$  to  $300^\circ$ , as presented in Figure 18.

## 6. Conclusions

PD experiments of the needle-plane defect in oil-paper insulation under AC-DC combined voltage are performed with 1:1, 1:3, 1:5 and 1:7 AC/DC proportions. Both PD parameters and PRPD patterns have been studied. The results of this paper show that AC/DC proportion has an obvious influence on PD characteristics, drawing the following conclusions:

- (1) PDIV and breakdown voltage increase with the decrease of AC/DC proportion;
- (2) Both pulse repetition rate and PD amplitude increases as the applied combined voltage increases throughout the whole PD process. The increase of DC component results in the decrease of PD occurrence rate and magnitude, including max PD amplitude, mean PD amplitude and total discharge amplitude;
- (3) At the initial stage, the distributions of PDs gradually develop toward the phase range between  $180^\circ$  and  $360^\circ$  as AC/DC proportion decreases. When it comes to the pre-breakdown stage, discharge pulses spread from  $0^\circ$  to  $360^\circ$ , with high-magnitude PDs only taking place around  $270^\circ$ .

PD characteristics under AC-DC combined voltage for needle-plane defects in oil-paper insulations are influenced by many complicated factors. Some papers [27,28] concerning the insulation diagnostic and condition monitoring in HVDC equipment based on partial discharge pattern recognition will contribute to the usage of results obtained in the current study. Mechanisms of PD behaviors under AC-DC combined voltage need further study.

**Acknowledgments:** The authors acknowledge the funding of China Electric Power Research Institute (GY71-15-048).

**Author Contributions:** Jiantao Sun contributed to the conception of the study. Xining Li performed the data analyses, wrote the manuscript and made corrections for the review. Lingyu Zhu contributed significantly to analysis and manuscript preparation. Shengchang Ji and Yanjie Cui helped perform the analysis with constructive discussions.

**Conflicts of Interest:** The authors declare no conflict of interest.

## References

1. CIGRE Joint Working Group. *HVDC Converter Transformers—Guide Lines for Conducting Design Reviews for HVDC Converter Transformers*; Technical Brochures A2/B4.28; International Council on Large Electric Systems: Paris, French, 2010.
2. Teague, W.L.; McWhirter, J.H. Dielectric measurements on new power transformer insulation. *IEEE Trans. Power Appar. Syst.* **1952**, *71*, 743–752.
3. International Electrotechnical Commission. *IEC 60270 High-Voltage Test Technique—Partial Discharge Measurements*; International Electrotechnical Commission: Geneva, Switzerland, 2000.
4. Bartnikas, R. Partial discharges: Their mechanism, detection and measurement. *IEEE Trans. Dielectr. Electr. Insul.* **2002**, *9*, 763–808. [[CrossRef](#)]
5. Montanari, G.C. Insulation diagnosis of high voltage apparatus by partial discharge investigation. In Proceedings of the 8th International Conference on Properties and Applications of Dielectric Materials, Bali, Indonesia, 26–30 June 2006.
6. Morshuis, P.H.F.; Smit, J.J. Partial discharge at DC voltage: Their mechanism detection and analysis. *IEEE Trans. Dielectr. Electr. Insul.* **2005**, *12*, 328–340. [[CrossRef](#)]
7. Wang, Y.H.; Wei, X.L.; Chen, Q.G.; Huang, Y.R.; Nie, H.Y. Breakdown characteristics of converter transformer insulation under composite AC and DC voltage. In Proceedings of the IEEE 9th International Conference on Properties and Applications of Dielectric Materials, Harbin, China, 19–23 July 2009; pp. 634–637.
8. Sarathi, R.; Koperundevi, G. UHF technique for Identification of partial discharge in a composite Insulation under AC and DC voltages. *IEEE Trans. Dielectr. Electr. Insul.* **2008**, *15*, 1724–1730. [[CrossRef](#)]
9. Sha, Y.; Zhou, Y.; Zhang, L.; Huang, M.; Jin, F. Measurement and simulation of partial discharge in oil-paper insulation under the combined AC-DC voltage. *J. Electrostat.* **2013**, *71*, 540–546. [[CrossRef](#)]

10. Takahashi, E.; Tsutsumi, Y.; Okuyama, K.; Ogata, F. Partial discharge characteristics of oil-immersed insulation systems under DC, combined AC-DC and DC reversed polarity voltage. *IEEE Trans. Power Appar. Syst.* **1976**, *95*, 411–420. [[CrossRef](#)]
11. Hao, M.; Zhou, Y.; Chen, G.; Wilson, G.; Jarman, P. Space charge behavior in oil gap and impregnated pressboard combined system under HVDC stresses. *IEEE Trans. Dielectr. Electr. Insul.* **2016**, *23*, 848–858. [[CrossRef](#)]
12. Li, J.; Liao, R.; Grzybowski, S.; Yang, L. Oil-paper aging evaluation by fuzzy clustering and factor analysis to statistical parameters of partial discharges. *IEEE Trans. Dielectr. Electr. Insul.* **2010**, *17*. [[CrossRef](#)]
13. Sha, Y.; Zhou, Y.; Li, J.; Wang, J. Partial discharge characteristics in oil-paper insulation under combined AC-DC voltage. *IEEE Trans. Dielectr. Electr. Insul.* **2014**, *21*, 1529–1539. [[CrossRef](#)]
14. Wu, H.; Li, C.; Qi, B.; Zhao, X.; Lv, J.; Zhao, L. The electric field distribution in oil-paper insulation under combined AC-DC voltage. In Proceedings of the IEEE International Conference on Condition Monitoring and Diagnosis, Bali, Indonesia, 23–27 September 2012; pp. 1097–1101.
15. Qi, B.; Wei, Z.; Li, C.; Gao, Y.; Zhang, X. Influences of different ratios of AC-DC combined voltage on internal gas cavity discharge in oil-pressboard insulation. *IEEE Trans. Power Deliv.* **2016**, *31*, 1026–1033. [[CrossRef](#)]
16. International Electrotechnical Commission. *IEC Standard 60641: Specification for Pressboard and Press-Paper for Electrical Purposes*; International Electrotechnical Commission: Geneva, Switzerland, 2008.
17. International Electrotechnical Commission. *IEC Standard 60243: Electrical Strength of Insulating Materials Test Methods*; International Electrotechnical Commission: Geneva, Switzerland, 1998.
18. IEEE Work Group. Recommended dielectric tests and test procedures for converter transformers and smoothing. *IEEE Trans. Power Deliv.* **1986**, *3*, 161–166.
19. IEEE Work Group. *IEEE Standard C57.129-2007: Standard for General Requirements and Test Code for Oil-Immersed HVDC Converter Transformers*; IEEE: New York, NY, USA, 2008.
20. Laughari, J.R. A short method of estimating life time of polypropylenes film using step-stress tests. *IEEE Trans. Dielectr. Electr. Insul.* **1990**, *25*, 1180–1182. [[CrossRef](#)]
21. Tang, L.C. Analysis of step-stress accelerated-life-test data: A new approach. *IEEE Trans. Reliab.* **1996**, *45*, 69–74. [[CrossRef](#)]
22. Li, J.; Han, X.; Liu, Z.; Yao, X.; Li, Y. PD characteristics of oil-pressboard insulation under AC and DC mixed voltage. *IEEE Trans. Dielectr. Electr. Insul.* **2016**, *23*, 444–450. [[CrossRef](#)]
23. Okubo, H.; Wakamatsu, M.; Inoue, N.; Kato, K.; Koide, H. Charge behavior in flowing oil in oil/pressboard insulation system by electro-optic field measurement. *IEEE Trans. Dielectr. Electr. Insul.* **2003**, *10*, 956–962. [[CrossRef](#)]
24. Chen, G. Research on the feature extraction of DC space charge behavior of oil-paper insulation. *Sci. China Technol. Sci.* **2011**, *54*, 1315–1324.
25. Radwan, R.M.; El-Dewieny, R.M.; Metwally, I.A. Investigation of static electrification phenomenon due to transformer oil flow in electric power apparatus. *IEEE Trans. Electr. Insul.* **1992**, *27*, 278–286. [[CrossRef](#)]
26. Ciobanu, R.; Schreiner, C.; Pfeiffer, W.; Baraboi, B. Space charge evolution in oil-paper insulation for dc cables application. In Proceedings of the IEEE 14th International Conference on Dielectric Liquids, Graz, Austria, 12 July 2002; pp. 321–324.
27. Majidi, M.; Fadali, M.S.; Etezadi-Amoli, M.; Oskuoee, M. Partial discharge pattern recognition via sparse representation and ANN. *IEEE Trans. Dielectr. Electr. Insul.* **2015**, *22*, 1061–1070. [[CrossRef](#)]
28. Majidi, M.; Oskuoee, M. Improving pattern recognition accuracy of partial discharges by new data preprocessing methods. *Electr. Power Syst. Res.* **2015**, *119*, 100–110. [[CrossRef](#)]

